PERGAMON

Electrochimica Acta 45 (1999) 351–367

ELECTROCHIMICA Acta

www.elsevier.nl/locate/electacta

Magnesium insertion electrodes for rechargeable nonaqueous batteries — a competitive alternative to lithium?

Petr Novák*, Roman Imhof[1], Otto Haas

Paul Scherrer Institute, Electrochemistry Section, CH-5232 Villigen PSI, Switzerland

Received 7 February 1999; received in revised form 12 March 1999

Abstract

Magnesium-based rechargeable batteries might be an interesting future alternative to lithium-based batteries. Here the available results of research, both on rechargeable negative electrodes based either on metallic magnesium or alternative materials, and on materials suitable as positive, magnesium-inserting (counter)electrodes for secondary magnesium batteries, are critically reviewed. The reversible magnesium-metal electrode was scarcely investigated and remains poorly understood. More data are available on host materials capable of reversible magnesium insertion, which are compared with lithium-inserting materials. © 1999 Elsevier Science Ltd. All rights reserved.

Keywords: Rechargeable magnesium batteries; Magnesium metal; Magnesium insertion; Lithium insertion; Insertion electrodes; Nonaqueous magnesium electrolytes; Review

1. Introduction

The need for new, high-performance battery systems is obvious when we consider the pace of expansion of human activity requiring mobile sources of electrical energy. The vast majority of current electrochemical studies is directed toward the promising lithium systems. But in view of the natural abundance of magnesium, its rather low equivalent weight (12 g per Faraday (F), as compared to 7 g/F for Li or 23 g/F for Na), its low price of ca $2700/ton [1] (metallic Li is currently about 24 times more expensive than metallic Mg [2]), and its safety characteristics, metallic magnesium should be examined as a potential alternative negative electrode for applications in which cost control is critical. Its electrode potential is less negative than that of lithium. More serious is the fact that magnesium electrochemistry at or near ambient temperature is rather poorly understood, and a substantial research effort will be required in order to develop competitive secondary magnesium electrodes [3,4].

In the following, the available results of research, both on rechargeable negative electrodes based on metallic magnesium and on materials suitable as positive, magnesium-inserting (counter)electrodes for secondary magnesium batteries are critically reviewed. Little relevant work has so far been published on rechargeable negative electrodes based on metallic magnesium, Mg alloys, or Mg^{2+} insertion materials. More data are available on materials suitable as positive, magnesium-inserting (counter)electrodes. The major part of this

* Corresponding author. Tel.: +41-563102457; fax: +41-563104415.

E-mail address: petr.novak@psi.ch (P. Novák)

[1] Present address. Renata AG, CH-4452 Itingen, Switzerland.

0013-4686/99/$ - see front matter
PII: S0013-4686(99)00216-9

Table 1
Characteristics of negative electrode materials (the values in parentheses are for the host without guest ions)

Electrode material	Molecular weight	Theoretical specific charge (Ah/kg)
Li	6.94	3862
Mg	24.31	2205
LiC_6 (graphite)	79.01 (72.07)	339 (372)
'MgC_6'	96.37 (72.07)	556 (744)

review will therefore focus on materials capable of magnesium insertion, and compare these data with results for lithium insertion electrodes.

2. Negative electrodes

Metallic lithium, lithium alloys, organic polymers, and various inorganic insertion materials were tested for their efficiency as negative electrodes of rechargeable lithium batteries. The theoretical specific charge of metallic lithium is higher than that of all other materials (Table 1). However, considering that the cycling efficiency of metallic lithium is never higher than 99%, and more often lower, one has to employ a multiple of the stoichiometric requirement of lithium in order to reach a satisfactory cycle life [5–7]. For this reason the practical specific charge of a secondary lithium electrode is much lower than the theoretical one, and comparable with the specific charges of alternative lithium-containing compounds such as LiC_6. Data on analogous, magnesium-based rechargeable negative electrodes are scarce [3,4,8,9]. However, the reasoning reported above for lithium remains valid for the magnesium case.

Reversible cycling of metallic magnesium in organic electrolytes seems to be quite difficult. It appears that Mg cannot be electrodeposited from most of the commonly used organic solutions [10,11], the exception being solutions based primarily on Grignard reagents (R-MgX, X=Br,Cl) [12–17]. In the past it was believed that the deposition from Grignard solutions does not yield sound, coherent deposits, and solutions based, e.g., on magnesium-boron complexes were suggested instead [18,19]. Alternative solutions for magnesium electrodeposition based on organometallic electrolytes containing CsF, $(C_2H_5)_2Mg$, $(C_2H_5)_3Al$, and $(iso\text{-}C_4H_9)_3Al$ in toluene were also developed [20]. However, recent work showed that compact layers containing ≥99.9% magnesium can be deposited at room temperature from ethyl or butylmagnesium bromide in tetrahydrofuran (THF) with added LiBr salt [21,22].

The electrodissolution of magnesium in nonaqueous electrolytes is also beset with difficulties because surface films render magnesium relatively inactive [23]. Without any precautions, high overpotentials are observed at current densities above 1 mA/cm^2 [24,25]. The films can be removed, e.g., by amalgamation [26] or by adding an acid to the organic electrolyte [27]. Saito et al. [28] published anodic polarization characteristics of Mg electrodes in some mixed organic electrolyte solutions based on $NaClO_4$ in formamide (FA), acetonitrile (AN), propylene carbonate (PC), THF, and dimethoxyethane (DME). The FA+AN (1:1 by vol.) solvent mixture was identified as the best one for Mg dissolution at rather low overpotentials, however, no data on Mg electrodeposition from this solution were given. It should be noted that the overpotential of magnesium dissolution is significantly increased when the nonaqueous electrolyte is contaminated with as little as 1% water [29]. Even more serious constraints exist in systems which contain traces of oxygen. The open-circuit potential of the metal shifts from ca 0.63 V vs Li/Li$^+$ [30] to ca 1.25 V vs Li/Li$^+$ [31] due to oxide formation. Moreover, the possible formation of insoluble magnesium superoxide means that significant anodic currents can be obtained only at potentials so far away from the Mg/Mg^{2+} equilibrium potential that oxygen reduction at the metal cannot take place [32].

Gregory et al. [3] and Hoffmann et al. [33] set out to identify electrolytes in which both Mg dissolution and deposition will occur at reasonable values of overpotential, and concluded that solutions of organomagnesium compounds in ethers or tertiary amines can be used. However, many of these are unstable in the presence of the transition metal oxides or sulfides used in the counterelectrode of the cell. Lossius and Emmenegger [4,34] studied the cyclability of metallic magnesium using magnesium salts in aprotic organic solvents, but the cycling efficiency of magnesium was insufficient in all electrolytes tested. The authors concluded that of the electrolytes tested, $Mg(CF_3SO_3)_2$ in dimethylacetamide is the most promising one, but even here considerable improvement is needed before a reversible Mg electrode useful in battery applications can be realized [4].

It is clear that the poor behavior of Mg electrodes is caused by passivation phenomena and surface film for-

mation processes [35]. Surface films effectively block the electrodes, as the mobility of the Mg^{2+} ions in the passivating films is extremely low [8,36]. Polymer and/or gel electrolytes might be useful to overcome this problem [37]; thus, using Mg complexes with fluorinated diketones, reversible plating/stripping of Mg was achieved from polyethylene oxide-based electrolytes [38]. Promising cyclability and reversibility of a secondary magnesium-polymer electrolyte cell using an electrolyte based on $MgCl_2$ and polyethylene glycol was claimed very recently [9].

Instead of depositing metallic magnesium (or, alternatively, producing magnesium-containing alloys) on a suitable substrate, there is also the possibility to insert Mg^{2+} ions into graphite or other suitable materials. The analogous insertion/de-insertion of Li^+ ions into/from carbon is the reversible reaction taking place in negative electrodes of commercially available lithium-ion cells; it was reviewed extensively in recent articles [39,40]. Data concerning magnesium insertion into carbons are scanty. Novák [41] attempted to intercalate Mg^{2+} ions into the graphite Timrex KS 6 using the electrolyte 1 M $Mg(ClO_4)_2$ in acetonitrile (both dry and with 1 M H_2O), but observed irreversible reactions only. Maeda et al. [42] and Maeda and Touzain [43] described reversible electrochemical insertion of Mg^{2+} ions into highly oriented pyrolytic graphite (HOPG) from $MgCl_2$ dissolved in dimethylsulfoxide, but solvent molecules (solv) were co-inserted into the graphite according to the reaction

$$Mg^{2+}(solv)_y + 2e^- + C_n \Leftrightarrow Mg(solv)_yC_n,$$

which implies both, low values of specific charge and short cycle life.

In summary, we can conclude that rechargeable negative electrodes for magnesium batteries were scarcely investigated, and remain poorly understood. Thus, competitive negative electrodes for magnesium-based systems are not available yet.

3. Positive electrodes

Numerous insertion/intercalation materials have been proposed for positive electrodes of rechargeable batteries [44].[2] Most of the work was devoted to the insertion of lithium and other alkali metal ions into host materials (see, for example, other contributions to this volume, conference proceedings [45,46], recent reviews [40,47], and references therein).

Positive electrode materials based on inorganic transition-metal oxides, sulfides, and borides are the only ones used up to now to insert magnesium ions. Fig. 1 compares the experimental potential ranges for reversible cycling of electrodes based on different materials. Fig. 1 which is based on published cyclic voltammograms and galvanostatic cycling curves (recalculated against the Li/Li^+ reference couple), indicates that in most cases the insertion of magnesium proceeds in the same potential region as the insertion of lithium. In fact, only one thermodynamic study exists showing that for the Mg^{2+} insertion into V_2O_5 aerogels the equilibrium electrode potential is 200–300 mV more positive than for the Li^+ insertion [48]. Generally speaking, sulfide-based electrodes show insertion potentials close to 2 V vs Li/Li^+. Oxide-based electrodes usually insert both, Mg^{2+} and Li^+ ions somewhere between 3 and 4.5 V vs Li/Li^+, but other insertion potentials were also observed.

In the following text we have divided the discussion of positive insertion electrode materials into Section 3.1, transition-metal sulfides; Section 3.2, transition-metal oxides; and Section 3.3, miscellaneous host materials.

3.1. Transition metal sulfides as insertion electrode materials

In Table 2 we have compiled what to our knowledge are all available results from chemical and electrochemical experiments dealing with the insertion of magnesium ions into transition metal sulfides, and compared them with the data for lithium insertion. The transition metal sulfides are widely regarded as

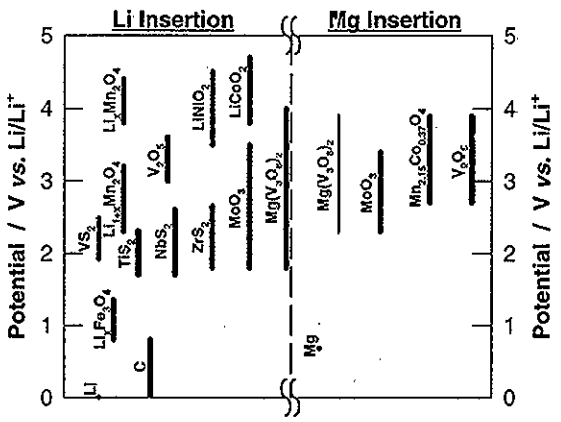

Fig. 1. Typical potential regions for the insertion of Li^+ and Mg^{2+} ions into various hosts.

[2] A common convention in the literature is that of regarding 'intercalation' as a special case of 'insertion'. The term 'intercalation' implies the restricting condition that a layered host matrix is involved in the intercalation process. Nevertheless, often both terms, insertion and intercalation, are used interchangeably.

Table 2
Transition metal sulfides used for chemical (c) and electrochemical (ec) insertion of lithium and magnesium ions, respectively[a]

Positive electrode material	Molecular weight	x_{max} in Li_xMS_y[b]		Ref.	x_{max} in Mg_xMS_y and experimental details			Ref.
		c	ec		c[c]	ec	Electrolyte	
TiS_2	112.01	1.0	~1.0	[49]	0.15	0.15	1 M $Mg(ClO_4)_2$/THF	[3]
TiS_2 cubic					0.25[d]			[53]
TiS_2 layered					0.22[d]			[53]
TiS_2						0.23	1 M $Mg(ClO_4)_2$ + 1.4 M H_2O/AN	[56]
ZrS_2	155.34	1.0	CV	[49]	0.66	0.66	1 M $Mg(ClO_4)_2$/THF	[3]
ZrS_2						0.16	1 M $Mg(ClO_4)_2$ + 1.4 M H_2O/AN	[56]
VS_2	115.06	See ref.	0.25 RT	[50]	0.34	0.34	1 M $Mg(ClO_4)_2$/THF	[3]
WS_2	247.91	0		[49]		0.28	$MgCl_2/AlCl_3$/EMIC, 80°C	[57]
MoS_2	160.06	1.5		[52]		0.96	$MgCl_2/AlCl_3$/EMIC, 80°C	[57]
Crystalline MoS_2			0.1	[51]				
Amorphous MoS_2			0.8	[51]				
NbS_2	157.03	0.78	See ref.	[49]		< 0.1	$MgCl_2/AlCl_3$/EMIC, 80°C	[57]
NbS_3	189.09		3	[62]		0.74	Mg-montmorillonite, 0.015 mA/cm^2	[63]
NbS_3		2.24		[58]		0.6	Mg-montmorillonite, 0.076 mA/cm^2	[63]

[a] CV, cyclic voltammogram; RT, room temperature; c, chemical insertion; ec, electrochemical insertion; THF, tetrahydrofuran; AN, acetonitrile; EMIC, 1-ethyl-3-methylimidazolium chloride.
[b] For experimental details see references.
[c] Di-*n*-butylmagnesium as reagent.
[d] Also with Mg-2,6-di-butylphenoxide as reagent.

prototype insertion/intercalation host materials. Chemical intercalation of lithium ions into two-dimensional layered transition metal disulfides of the general type MX_2 (M = Ti, Zr, Hf, Nb, Ta, Mo, W, V and X = S) is therefore well documented [49–52]. A convenient lithium source used to perform the intercalation reaction smoothly is n-butyllithium (see, e.g., the references in [49]). There are also several reports on the electrochemical intercalation of lithium into the same host structures [49,50]. For example, over 400 electrochemical intercalation/de-intercalation cycles with only 20% overall loss in electrode utilization have been demonstrated for Li_xTiS_2 [49]. The reaction mechanism of lithium ion intercalation was suggested [49] to be represented by the following equation:

$$Li^+ + e^- + Ti^{4+}(S^{2-})_2 \Leftrightarrow (Li^+)Ti^{3+}(S^{2-})_2.$$

The intercalation of Mg^{2+} ions into these host structures has received only limited attention up to now. There are two studies, by Gregory et al. [3] concerning chemical Mg^{2+} intercalation into TiS_2, VS_2, and ZrS_2, and by Bruce et al. [53] concerning chemical intercalation into TiS_2. For TiS_2 two structural studies of the magnesium-intercalated samples exist [54,55]. Gregory et al. [3] also screened the electrochemical Mg^{2+} intercalation using a 1 M $Mg(ClO_4)_2$ solution in tetrahydrofuran (THF), and claimed to have obtained intercalation levels comparable with those attained by the chemical treatment.[3] Novák and Desilvestro [56] pointed out that the water content in the electrolyte plays an important role in the intercalation reactions. For their electrochemical intercalation experiments they used dry acetonitrile (AN), in which the $Mg(ClO_4)_2$ is better soluble than in THF, but detected electrochemical activity, neither for ZrS_2 nor for TiS_2 using this dry electrolyte. In wet electrolytes based on THF, propylene carbonate (PC), and AN they only observed irreversible reduction of the sulfides. The use of a molten-salt electrolyte based on $MgCl_2/AlCl_3$/1-ethyl-3-methylimidazolium chloride (EMIC) at 80°C in combination with WS_2, MoS_2, and NbS_2 also failed to bring about reversible Mg^{2+} intercalation [57].

Another class of materials used to insert lithium and magnesium cations are the transition metal trichalcogenides of the general formula MX_3, which show a pseudo-one-dimensional structure where trigonal prismatic $[MX_6]$ units share their upper and lower faces. The $[MX_6]$ chains are weakly bonded with each other and the guest cations are assumed to be inserted into the interchain spaces [58]. The overall reaction of lithium ion insertion was suggested to be represented

[3] Anhydrous $Mg(ClO_4)_2$ is rather insoluble in dry THF containing ca 70 ppm H_2O [56]. However, the solubility of $Mg(ClO_4)_2$ in THF can be increased by increasing the H_2O concentration in the solvent. H_2O may either be added, or be introduced from $Mg(ClO_4)_2$ containing crystalline H_2O. We therefore suppose that the authors of reference [3] worked with a 'wet' 1 M solution of $Mg(ClO_4)_2$ in THF. Thus, the results from reference [3] cited in the text and Tables 2–6 should be interpreted cautiously.

by the following two equations [59]:

$$2Li^+ + 2e^- + M^{4+}X^{2-}X_2^{2-} \Leftrightarrow (Li^+)_2M^{4+}(X^{2-})_3,$$

$$Li^+ + e^- + (Li^+)_2M^{4+}(X^{2-})_3 \Leftrightarrow (Li^+)_3M^{3+}(X^{2-})_3.$$

The dimer X—X is reduced in a first reaction step, which is followed by the reduction of the transition metal itself. Three lithium ions can theoretically be inserted into one MX_3 unit.

An interesting insertion material is NbS_3, which can have either a triclinic [60] or a monoclinic structure. The latter can be obtained under high pressure [61] and shows three slightly different X—X distances in a unit cell, in contrast to the triclinic modification. Yamamoto et al. [62] compared the lithium-ion intercalation behavior of the triclinic NbS_3 with the monoclinic modification, while Yuan and Günter [63] performed electrochemical magnesium insertion studies on the monoclinic material.

In the case of galvanostatic Li^+ intercalation, the monoclinic modification shows two potential plateaus at about 1.8 and 1.3 V vs Li/Li^+, corresponding to Li_xNbS_3 with $x \leq 1.7$ and $x = 2.2$–2.8, respectively. In contrast to this behavior, the potential of the triclinic material decreases gradually over the composition region from $x = 0.3$ to $x = 1.7$. For the latter lithium content a potential of ca 1.4 V vs Li/Li^+ is observed, which then remains almost constant during further lithium insertion over the whole composition range from $x = 1.7$ to $x = 2.5$. The electrode potential of the monoclinic NbS_3 is more positive than that of the triclinic NbS_3 up to $x = 2$ [62]. The capacity fade during cycling was very important for both modifications. In addition, a structural transformation from monoclinic to an unknown structural phase seems to occur at $x > 2$.

In the case of Mg^{2+} insertion into NbS_3, the open-circuit voltage (OCV) of a cell having a solid electrolyte and a metallic Mg counterelectrode was 1.82 V. During the first galvanostatic Mg^{2+} insertion half-cycle a flat voltage plateau was observed at about 1.48 V for compositions from $x > 0$ to $x = 0.46$ in Mg_xNbS_3. A second voltage plateau was observed at about 1.2 V over the composition range $x = 0.48$–0.58. The cell voltage then gradually decreased to 1 V at $x = 0.6$ [63]. No structural change was detected for the composition $Mg_{0.6}NbS_3$. The insertion reaction was hardly reversible, however, cycling results for up to five cycles were reported.

In conclusion, in contrast to the insertion of lithium ions into transition metal sulfides the electrochemical Mg^{2+} insertion into these compounds is difficult and hardly reversible.

3.2. Oxides as insertion electrode materials

Oxides are considered to be the most promising positive electrode materials for high-energy-density secondary lithium batteries. The reason resides in the high degree of ionic character of the metal-oxygen bond in oxides, which generally leads to a high oxidizing power of the compound and hence to a high voltage of the battery [64]. Moreover, oxides usually have a much higher chemical stability than sulfides. This is an advantage in battery applications because of the expected longer cycle life of oxide-based electrodes. Numerous oxides are suitable as hosts for lithium insertion [40]. However, only a few of them were tested as well for magnesium insertion, and are discussed further. The results of chemical and electrochemical insertion experiments on oxides are summarized in Tables 3–5.

3.2.1. V_2O_5

The highest oxides of vanadium, chromium, niobium, as well as molybdenum are well known for their ability to electrochemically insert large amounts of lithium. However, mostly due to a limited cycling stability of other oxides, so far only the vanadium oxides V_2O_5 and V_6O_{13} have gained importance as rechargeable '3 V' electrode materials in lithium cells.

As an oversimplification, V_2O_5 can be regarded as a layered structure [65] similar to that of TiS_2. The description of the V_2O_5 structure (Fig. 2) is based on square-pyramidal coordination of V^{5+} with five oxygens and a weak V—O interaction with the sixth oxygen. The long V—O bonds normal to the *ac* plane facilitate mica-like cleavage parallel to that plane, so that the inclusion of alkali and other metals is possible [66].

Whittingham in 1975 [67] reported the reversible electrochemical lithium insertion into V_2O_5 at room

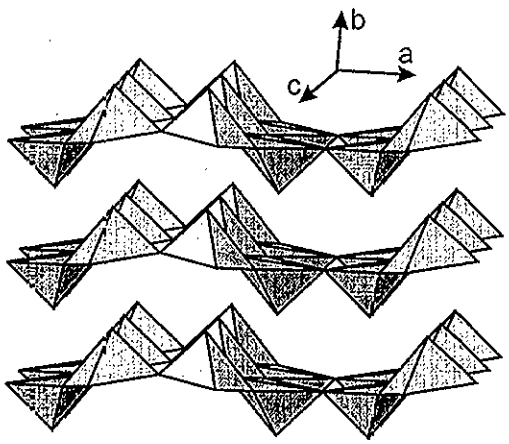

Fig. 2. The crystal structure of V_2O_5.

Table 3
Vanadium oxides used for chemical (c) and electrochemical (ec) insertion of lithium and magnesium ions, respectively[a]

Positive electrode material	Molecular weight	x_{max} in $Li_xM_yO_z$ [b] c	ec	Ref.	x_{max} in $Mg_xM_yO_z$ and experimental details c[c]	ec	Electrolyte	Ref.
V_2O_5	181.88					0.5	$Mg(ClO_4)_2$ in $DMSO_2$ or sulfolane, 150°C	[71]
					0.66	0.66	1 M $Mg(ClO_4)_2$/THF	[3]
					0.10			[53]
							1 M $Mg(ClO_4)_2$/AN or PC or triglyme	
						< ?	(< 1000 ppm H_2O)	[56]
						0.58	1 M $Mg(ClO_4)_2$ + 1 M H_2O/AN	[56]
						0.58	1.7 M $Mg(ClO_4)_2$ + 6 M H_2O/THF	[56]
V_2O_5 aerogel		4.0		[78]	2.0	0.6	0.1 M $Mg(CF_3SO_3)_2$/PC	[48]
$M_aV_3O_8$	280.82		3.46	[96]		0.79	0.5–1.0 M $Mg(ClO_4)_2$ + 0.5–2.0 M H_2O/AN	[96]
							1.0 M $Mg(ClO_4)_2$/PC(< 50 ppm H_2O)	
							$MgCl_2/AlCl_3$/EMIC, 80°C	
V_6O_{13}	513.64				0.48			[53]
						3.64	1 M $Mg(ClO_4)_2$ + 1 M H_2O/AN	[87]

[a] c, chemical insertion; ec, electrochemical insertion; THF, tetrahydrofuran; $DMSO_2$, dimethylsulfone; AN, acetonitrile; PC, propylene carbonate; EMIC, 1-ethyl-3-methylimidazolium chloride.
[b] For experimental details see references.
[c] Di-*n*-butylmagnesium as reagent.

temperature. It was believed over a long period of time that a lithium content of $x = 1$ in $Li_xV_2O_5$ cannot be exceeded without losing the reversibility of the insertion process. Later it could be shown that at lithium contents $x > 1$ a structural modification occurs, and that the new phase can be reversibly cycled in the stoichiometric range $0 \leq x \leq 2$ [68,69]. Insertion of a third lithium into V_2O_5 irreversibly leads to the formation of the so-called ω-phase with a rock-salt type structure. Almost all the lithium from the ω-phase can be electrochemically de-inserted, so that this phase constitutes a unique positive electrode material for secondary lithium batteries which yield specific energies of up to 900 Wh/kg. For an ω-$Li_xV_2O_5$/Li cell, 100 cycles with more than 450 Wh/kg have been demonstrated in a voltage range between 3.4 and 1.9 V [64,70].

The good lithium insertion properties of V_2O_5 triggered exploratory research into other cationic guests, in particular Mg^{2+} ions. Chemical insertion tests with dibutylmagnesium reagent (Table 3) revealed that compositions from $Mg_{0.1}V_2O_5$ to as high as $Mg_{0.66}V_2O_5$ are possible [3,53]. Pereira-Ramos et al. [71] reported the reversible electrochemical insertion of Mg^{2+} into V_2O_5 at 150°C from $Mg(ClO_4)_2$ solutions in molten dimethylsulfone or sulfolane according to

$$x\mathrm{Mg}^{2+} + 2x\mathrm{e}^- + \mathrm{V_2O_5} \Leftrightarrow \mathrm{Mg}_x\mathrm{V_2O_5}.$$

At a current density of 0.1 mA/cm^2 they reached the composition $Mg_{0.5}V_2O_5$. Their X-ray diffraction experiments indicated that the structure of the $Mg_xV_2O_5$ phase formed electrochemically was closely related to that of the parent oxide V_2O_5. Unfortunately, the reversibility of the electrochemical reaction was limited to a few cycles [71].

The reversible cycling of polycrystalline V_2O_5 in Mg^{2+}-containing electrolytes at room temperature was reported by Novák and Desilvestro [56] (Fig. 3). The amount of electrochemically inserted Mg^{2+} depends on the amount of H_2O in the electrolyte.[4] The highest

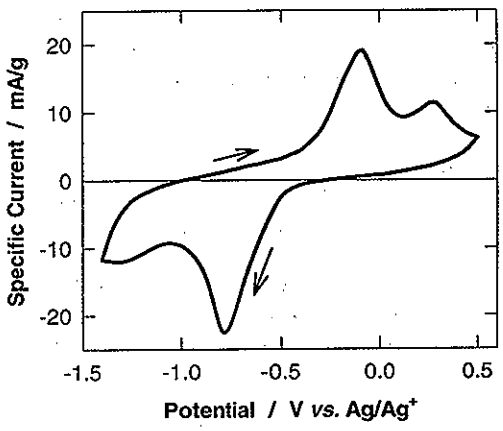

Fig. 3. A cyclic voltammogram of V_2O_5 in the electrolyte 1 M $Mg(ClO_4)_2$ + 1 M H_2O in acetonitrile [56].

[4] Recall that for the anodic reaction water is detrimental: the overpotential of electrodissolution of metallic magnesium increases significantly when the nonaqueous electrolyte is contaminated with as little as 1% water, as discussed in Section 2.

specific charge, of 170 Ah/kg, was attained in a 1 M $Mg(ClO_4)_2$ + 1 M H_2O solution in acetonitrile (AN). However, the cycling stability of the electrode was not sufficient — after 20 cycles only about 50 Ah/kg were available.

A crystallographic study of $Mg_xV_2O_5$ revealed that (i) both the chemical and electrochemical Mg^{2+} insertion into V_2O_5 produces similar V_2O_5-related phases, (ii) the electrochemically inserted product $Mg_xV_2O_5$ obtained in wet acetonitrile has a multiphase character, and (iii) the content of one of the $Mg_xV_2O_5$ phases in the electrode decreases during electrochemical cycling [72]. Moreover, the rather smooth surface of the V_2O_5 crystals becomes rough after electrochemical Mg^{2+} insertion, and the diffusion of Mg^{2+} ions into the bulk V_2O_5 is slow and incomplete [73]. The Mg^{2+} insertion into the bulk is strongly hindered, probably due to the formation of surface layers consisting, e.g., of some irreversible reaction products and containing species like MgO [73]. The existence of ten different phases (most of them solid solutions) was postulated in a Mg-V_2O_5 phase diagram published by Galy and Pouchard [74]. The same group concluded that the width of homogeneity ranges of the $M_xV_2O_5$ phases depends on the charge of the inserted element, M, and its insertion rate [75]. Thus, it is clear that under the conditions expected in a real Mg battery, Mg^{2+} insertion into V_2O_5 would represent a very complex process.

Besides crystalline V_2O_5, promising results for ion insertion have been reported for V_2O_5 glasses with P_2O_5 or other network formers, V_2O_5 xerogels, and V_2O_5 aerogels [76,77]. These amorphous or poorly crystalline materials offer considerable advantages by virtue of their morphology. The large electrochemically active surface area, small particle size, and low density lead to high overall diffusion coefficients and at the same time to low volume expansion during ion insertion. Amorphous V_2O_5 aerogels with high surface area, consisting of interpenetrating networks of water and V_2O_5 rods, coils, and ribbons, can host at least 4 moles of Li^+ per mole of V_2O_5 [78,79]. For lithium cells with a xerogel positive electrode specific energies of over 700 Wh/kg were measured [80]. However, limited long-term cycling stability has been a major problem with such electrode materials so far.

The capacity of the V_2O_5 aerogels for the chemical insertion of polyvalent cations is comparable to that for the insertion of Li^+ ions [48]. Thus, two moles of Mg^{2+} per mole of V_2O_5 can be inserted *chemically*, which formally corresponds to the reduction of pentavalent vanadium to the trivalent state [48]. This is the highest Mg^{2+} insertion capacity ever reported for any vanadium oxide host. From this figure the authors estimated that a specific energy (based on the mass of active cathode material) of 1200 Wh/kg is possible for a hypothetical Mg/V_2O_5-aerogel cell [48]. However, in *electrochemical* experiments the maximum Mg content was less than $Mg_{0.6}V_2O_5$ [48]. Moreover, the chemically bound water is a potential drawback of the V_2O_5 aerogels or xerogels, because hydrate compositions of up to $V_2O_5.5H_2O$ are possible [81]. Based on an X-ray diffraction study, Bouhaouss et al. [82] suggested that for each Mg-containing layer two layers of water molecules exist in the crystal structure of $Mg_xV_2O_5.nH_2O$. At least for Li^+, though, Le et al. [48] found that fortunately the chemically bound water did not react with the inserted metal in their aerogels having a composition of $V_2O_5.0.4H_2O$.

3.2.2. V_6O_{13}

The oxide V_6O_{13} was first reported as a positive electrode material for lithium insertion by Murphy et al. [83,84]. Up to 8 Li^+ per formula unit can be chemically inserted into stoichiometric V_6O_{13} using butyllithium, and even more can be inserted into non-stoichiometric V_6O_{13+z} [85]. However, only up to 6 Li^+ can be reversibly inserted into V_6O_{13} electrochemically [86].

Bruce et al. [53] investigated the chemical insertion of Mg^{2+} into V_6O_{13} and concluded that, at a composition of $Mg_{0.48}V_6O_{13}$, this oxide could appear to accommodate a high magnesium content; but relative to the number of vanadium ions, the Mg^{2+} content is in fact rather low. Joho [87] and Joho et al. [88] demonstrated a reversible electrochemical cycling of V_6O_{13} in Mg^{2+}-containing electrolytes. As in the V_2O_5 case, the amount of electrochemically inserted Mg^{2+} depends on the water concentration in the electrolyte. Specific charges of up to 380 Ah/kg were attained for the insertion process in an acetonitrile solution containing 1 M $Mg(ClO_4)_2$ and 1 M H_2O. However, the specific charge significantly decreased during cycling. In addition, a partial insertion of H^+ parallel to the insertion of Mg^{2+} in wet $Mg(ClO_4)_2$ solutions cannot be excluded in view of experiments in H_2O-containing Bu_4NClO_4 electrolytes [87,88].

3.2.3. $M_aV_3O_8$

The vanadates (often called vanadium bronzes) $Li_{1+x}V_3O_8$ [89–91], $Na_{1+x}V_3O_8$ [92,93], and $Mg(V_3O_8)_2$ [94–96] are examples of layered insertion compounds in which the alkaline or alkaline earth metal atoms function as spacers between the vanadium oxide units. These spacers stabilize the oxide structure during the insertion/de-insertion process and optimize the spacing between the vanadium oxide units. This enhances, not only the amount of insertable guest species but also the ion diffusion rate, both effects leading to a superior electrode performance. A specific charge for lithium insertion of more than 300 Ah/kg has been reported for these bronzes [92,97,98]. Compounds $Li_{3.8}V_3O_8$ [97,99] and $Li_3NaV_3O_8$ [98] pro-

duced by chemical lithiation can be used as positive electrode materials constituting the lithium source in cells with carbon as the negative electrode. A stable specific charge of 210 Ah/kg has been demonstrated for more than 100 cycles with $Li_3NaV_3O_8$ [98].

Vanadium bronzes containing chemically bound water, $MV_3O_8(H_2O)_y$ (M = Li, Na, K, $Ca_{0.5}$, or $Mg_{0.5}$), are layered, poorly crystalline materials [72]. They are superior hosts for Mg^{2+} insertion [94–96]. In acetonitrile-based electrolytes maximum specific charges of ~200 Ah/kg were measured, but the charge decreased rapidly with increasing cycle number [95]. A salt melt (liquid at room temperature) based on $MgCl_2$, $AlCl_3$, and 1-ethyl-3-methylimidazolium chloride offers an interesting alternative to common aprotic electrolytes (Fig. 4). It is possible to insert Mg^{2+} electrochemically from the salt melt into the bronzes [94–96]. Except for the first few cycles, the behavior of all bronzes is similar in this electrolyte. A steady state is reached after about five cycles, and a reversible insertion and extraction of Mg^{2+} is observed for all bronzes. Specific charges of up to 150 Ah/kg for Mg^{2+} insertion were measured in the first cycle, and >80 Ah/kg can be utilized during 60 deep cycles [95]. Variations in the content of bound lattice water in the bronzes are responsible for differences in the electrochemical properties [94]. The presence of this water seems to be essential [95]. Unfortunately, all lattice water is removed during cycling [96].

3.2.4. MoO_3

Orthorhombic MoO_3 is a known intercalation host for diverse monovalent and multivalent cations. The intercalation properties of MoO_3 are due to its unique layer structure [100] as shown in Fig. 5. Edge and corner-sharing [MoO_6] octahedra build up double layers. These layer planes are held together by weak van der Waals attraction forces. Guest ions like Li^+ or Mg^{2+} are easily accommodated between the layers, the layers are preserved during intercalation/de-intercalation cycles.

Lithium can be intercalated into MoO_3 chemically [101] or electrochemically [102]. Since electrochemical intercalation/de-intercalation cycles of Li^+ into/from MoO_3 are reversible, an application of this material in both secondary lithium batteries and electrochromic devices has been suggested [103–105], but the relatively low specific energy of the Li/MoO_3 couple and the poor cycling stability of the oxide constitute recognized drawbacks.

The intercalation of lithium into MoO_3 has been thoroughly investigated, and the reaction mechanism seems to be well understood [106–108]. During the initial reduction, a part of the intercalated lithium is irreversibly trapped in the oxide, and $Li_{z+x}MoO_3$ is formed. During re-oxidation and subsequent cycles,

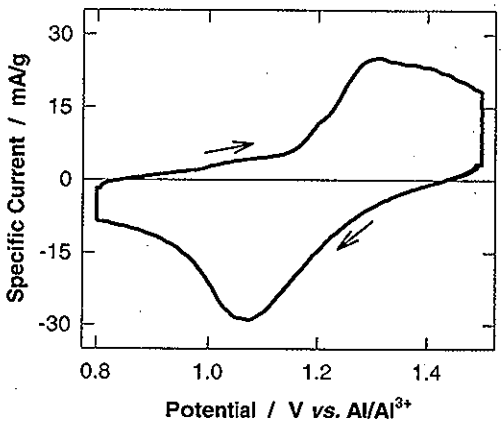

Fig. 4. A cyclic voltammogram (30th cycle) of $Mg(V_3O_8)_2$ in the electrolyte $MgCl_2 + AlCl_3 + EMIC$ at 80°C [95].

only x moles of lithium are de-intercalated and re-inserted. A complete lithium extraction is not possible. Thus, the electrochemical reactions can be described as

$$(z+x)Li^+ + (z+x)e^- + MoO_3 \rightarrow Li_{z+x}MoO_3$$

for initial reduction and

$$xLi^+ + xe^- + Li_zMoO_3 \Leftrightarrow Li_{z+x}MoO_3$$

for cycling. The kinetically accessible stoichiometric range of the reversible lithium intercalation/de-intercalation is $0.1 < y < 1.5$ in Li_yMoO_3 ($y = z + x$) [106]. The intercalation of lithium causes an increase of the interlayer distance because of the repulsion forces

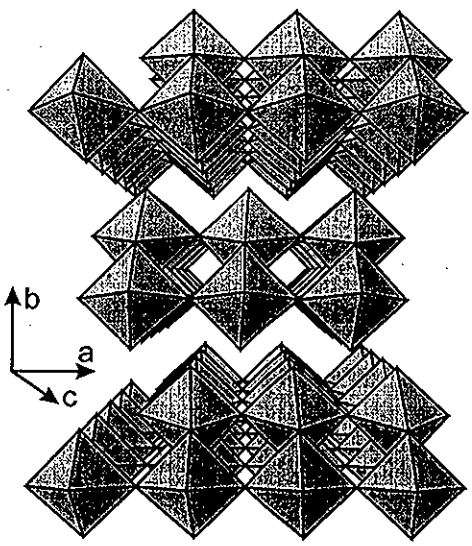

Fig. 5. The crystal structure of MoO_3.

Table 4
Molybdenum oxide used for chemical (c) and electrochemical (ec) insertion of lithium and magnesium ions, respectively[a]

Positive electrode material	Molecular weight	x_{max} in Li_xMoO_3[b] c	ec	Ref.	x_{max} in Mg_xMoO_3 and experimental details c[c]	ec	Electrolyte	Ref.
MoO_3	143.94		1.61	[109]	0.50	0.50	1 M $Mg(ClO_4)_2$/THF	[3]
		1 55		[101]	0.05			[53]
			1.5	[106]		0.43	$MgCl_2/AlCl_3$/EMIC, 80°C	[109]
				[106]		0.56	1 M $Mg(ClO_4)_2$+1.5 M H_2O/AN	[109]
				[103]				

[a] c, chemical insertion; ec, electrochemical insertion; THF, tetrahydrofuran; AN, acetonitrile; EMIC, 1-ethyl-3-methylimidazolium chloride.
[b] For experimental details see references.
[c] Di-*n*-butylmagnesium as reagent.

between the intercalated cations and the host cations. This lattice expansion has a maximum for $y = 0.5$ in Li_yMoO_3 and leads to cracking of the MoO_3 crystals during intercalation and, thus, to a decrease in particle size [106]. As a result MoO_3 is cycled in a quasi-amorphous state.

Specific charges of up to 300 Ah/kg were obtained in organic, propylene carbonate-based electrolytes for the lithium intercalation into MoO_3 [109]. The specific charge decreased to ca 250 Ah/kg after 12 cycles. In Table 4 the data for lithium intercalation into MoO_3 are summarized and compared with magnesium intercalation.

Analogously to the lithium case, the host properties of MoO_3 admit the electrochemical intercalation of divalent magnesium cations [109,110]. From *chemical* intercalation tests in a solution of dibutylmagnesium in heptane as intercalation reagent, a potential specific charge of about 140 Ah/kg (corresponding to a stoichiometry of $Mg_{0.5}MoO_3$) was estimated by Gregory et al. [3]. However, another group, also using the dibutylmagnesium/heptane solution, measured a 10 times lower magnesium content after chemical intercalation, thus obtaining $Mg_{0.05}MoO_3$ [53].

Reversible electrochemical Mg^{2+} intercalation from dry electrolytes into MoO_3 was demonstrated using a room temperature molten-salt electrolyte consisting of 3 wt% $MgCl_2$, 56 wt% $AlCl_3$, and 41 wt% 1-ethyl-3-methylimidazolium chloride [109,110]. A specific charge of ca 160 Ah/kg was obtained in the first intercalation half-cycle. As in the case of V_2O_5, the Mg^{2+} intercalation process is enhanced in organic electrolytes with traces of H_2O. The cyclic voltammogram changes substantially during cycling (Fig. 6); this reflects the above mentioned transformation of MoO_3 from crystalline to the quasi-amorphous state. In 1 M $Mg(ClO_4)_2$ in acetonitrile (AN) with 1.5 M H_2O, specific charges for Mg^{2+} insertion of up to 210 Ah/kg were measured during the first reduction of the oxide [109]. However, in both electrolytes the specific charge decreases with the cycle number. After ten cycles, it has fallen to ca 150 Ah/kg in wet AN and to ca 50 Ah/kg in molten salts.

3.2.5. Other oxides

Spinel materials of the general formula AM_2O_4 are very popular insertion hosts. The crystal structure of a spinel consists of alternate rows of MO_6 octahedra and metal ions, A, in positions of tetrahedral coordination (Fig. 7), and possesses a three-dimensional lattice with cross-linked channels suitable for cation insertion. The theoretical advantages of such three-dimensional frameworks over two-dimensional layered structures are (i) the possibility of avoiding, for steric reasons, the co-insertion of bulky species such as solvent molecules, and (ii) the smaller degree of expansion/contraction of the structure upon ion insertion/de-insertion. An

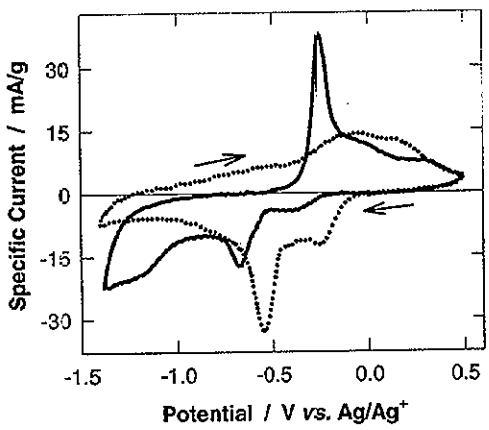

Fig. 6. Cyclic voltammograms of MoO_3 in the electrolyte 1 M $Mg(ClO_4)_2$+1.5 M H_2O in acetonitrile [109]; (—) first cycle, (...) fifth cycle.

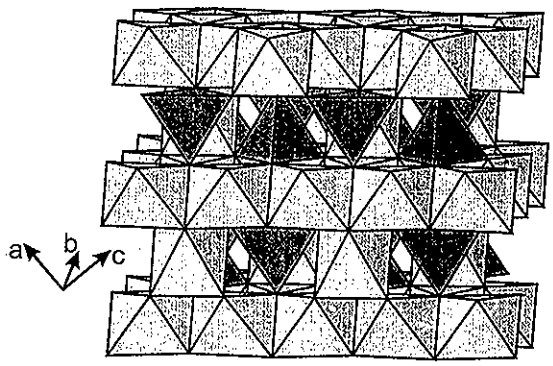

Fig. 7. The three-dimensional spinel framework.

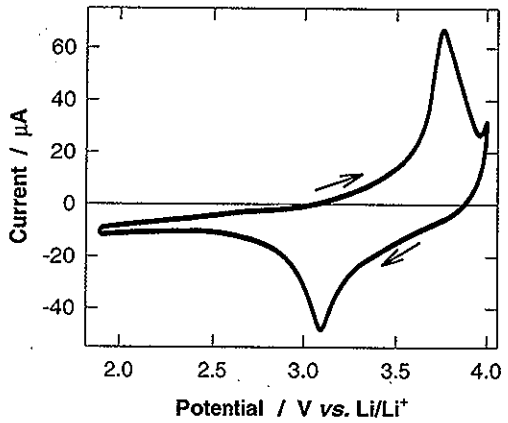

Fig. 8. A cyclic voltammogram of $Mn_{2.15}Co_{0.37}O_4$ in the electrolyte 0.1 M $Mg(ClO_4)_2$ in propylene carbonate [111].

immense variety of spinel samples have been screened for their possible application in lithium-ion batteries. However, only a few of these materials have been tested with magnesium, and will be discussed here. The data are included in Table 5.

The electrochemical insertion of Mg^{2+} into the cation-deficient, mixed oxide $Mn_{2.15}Co_{0.37}O_4$ was recently studied by Sánchez and Pereira-Ramos [111]. X-ray diffraction studies revealed a tetragonal spinel structure of this oxide, which was retained upon insertion of 0.23 Mg^{2+} per mole of oxide. Electrochemical measurements were performed in a three-electrode setup with a magnesium counterelectrode and a lithium reference electrode separated by a thin porous frit from the electrochemical cell. The spinel shows a reversible insertion process at a potential of ca 3.1 V vs Li/Li^+ (Fig. 8) and a rather stable specific charge of ca 30 Ah/kg (C/6, 4.05–1.85 V vs Li/Li^+) (Table 5). However, the magnesium uptake of $Mn_{2.15}Co_{0.37}O_4$ is considerably lower than the analogous figure found for lithium insertion (x in $Li_xMn_{2.15}Co_{0.37}O_4 = \approx 0.62$) [112,113].

Three other spinels were included in the comprehensive study of magnesium insertion performed by Gregory et al. [3]. The binary spinels Co_3O_4, Mn_3O_4,

Table 5
Other metal oxides used for chemical (c) and electrochemical (ec) insertion of lithium and magneisum ions, respectively[a]

Positive electrode material	Molecular weight	x_{max} in $Li_xM_yO_z$[b]		Ref.	x_{max} in $Mg_xM_yO_z$ and experimental details			Ref.
		c	ec		c[c]	ec	Electrolyte	
RuO_2	133.07	> 1.0		[65,115]	0.66	0.66	1 M $Mg(ClO_4)_2$/THF	[3]
						< 0.1		[56]
Co_3O_4	240.79			[133]	0.80	0.80	1 M $Mg(ClO_4)_2$/THF	[3]
						< 0.1		[56]
WO_3	231.85	< 1.5		[65]	0.50	0.50	1 M $Mg(ClO_4)_2$/THF	[3]
			1.1	[134]	0.08			[53]
γ-MnO_2	86.94				0.32			[53]
λ-MnO_2	86.94				0.09			[53]
β-MnO_2	86.94				0.02			[53]
Mn_2O_3	157.88				0.66	0.66	1 M $Mg(ClO_4)_2$/THF	[3]
Mn_3O_4	228.82			[133]	0.66	0.66	1 M $Mg(ClO_4)_2$/THF	[3]
$Mn_{2.15}Co_{0.37}O_4$	203.93	0.62	0.7	[112]		0.23	0.1 M $Mg(ClO_4)_2$/PC	[111]
PbO_2	239.19				0.25	0.25	1 M $Mg(ClO_4)_2$/THF	[3]
Pb_3O_4	685.57				0.25	0.25	1 M $Mg(ClO_4)_2$/THF	[3]
U_3O_8	842.09	0.87	2.07	[115,135]	0.50	0.78	1 M Mg $(ClO_4)_2$/DMF	[115]

[a] c, chemical insertion; ec, electrochemical insertion; THF, tetrahydrofuran; PC, propylene carbonate; DMF, dimethylformamide.
[b] For experimental details see references.
[c] Di-*n*-butylmagnesium as reagent.

and Pb_3O_4 were tested for chemical and electrochemical magnesium insertion, as were the oxides RuO_2, WO_3, Mn_2O_3, and PbO_2. All these samples revealed considerable magnesium uptake according to this study (Table 5). As an example, RuO_2 was shown to have an initial discharge potential plateau at about 2.2 V, inserting 0.66 M magnesium ions into the structure. This process was claimed to be fully reversible. A second plateau at 2 V follows, however, this leads to the irreversible disproportionation of the material to MgO and Ru. Nevertheless, some disagreement with later studies seems to exist. Whereas reference [3] reports the successful electrochemical insertion of 0.66 and 0.8 M of Mg^{2+} ions per mole of oxide into RuO_2 and Co_3O_4, respectively, Novák and Desilvestro [56] report no electrochemical activity in dry organic electrolytes, and only irreversible reduction in THF, PC, and AN-based wet electrolytes. A second disagreement consists in the x-value of the chemical magnesium insertion into WO_3, which is reported to be 0.5 M per mole of oxide in the study of Gregory et al. [3] but only 0.08 M per mole of oxide according to Bruce et al. [53].

Another insertion material is α-U_3O_8, which was studied using both lithium and magnesium ions. This substance has a pillared layer structure consisting of edge-sharing UO_5 pentagons connected by perpendicular U—O—U chains [114]. Electrochemical measurements reveal four single-phase regions for $Li_xU_3O_8$ between $x = 0.78$ and $x = 2.07$. According to X-ray powder diffraction the lithium insertion into this material was said to cause very little change in the parent crystal structure over the whole x-range [115]. Ion insertion occurs between the pentagonal layers, causing a slight expansion in the c-direction. The maximum x-value achieved electrochemically for magnesium insertion was reported to be 0.78 [115]. Ambient temperature discharge curves indicated the presence of two single-phase regions at $0.20 < x < 0.27$ and $x > 0.40$. At 100°C, the positions of the single phase regions shifted to higher x-values, and the insertion of magnesium into U_3O_8 increased. The experiments were performed in a $Mg(ClO_4)_2$/dimethylformamide-based electrolyte. Attempts to charge the electrode after discharge showed the insertion process to be reversible. Chemical and self-diffusion coefficients were also estimated using a current pulse method, and found for magnesium to be two to three orders of magnitude lower than those for lithium in $Li_xU_3O_8$.

3.3. Miscellaneous insertion electrode materials

Some results were reported about the chemical and electrochemical insertion of Mg^{2+} into three different borides, namely MoB_2, TiB_2, and ZrB_2 [3], which are summarized in Table 6. However, no further information about these experiments was given in the original paper.

4. Electrolytes for rechargeable magnesium batteries

Electrolyte solutions compatible with either the negative *or* positive electrode are mentioned in the appropriate chapters as well as in Tables 2–6. For complete cells the electrolytes tested include the solution of magnesium dibutyldiphenylborate in THF/DME [31] as well as Mg^{2+}-conducting polymer and solid electrolytes [9]. Reports dealing chiefly with nonaqueous electrolytes suitable for near-ambient-temperature magnesium batteries are scarce. Lossius and Emmenegger [4,34] investigated the conductivity of electrolyte solutions prepared from nine magnesium salts in 20 aprotic organic solvents (N-and O-donors) and 70 of their mixtures. Detailed data are available from an internal report [34]; a compact summary of the results was published later [4]. Liebenow [116] provided some data on a novel type of magnesium-ion-conducting polymer electrolyte. There is also a study dealing with ionic conduction of magnesium salts in organized smectic liquid-crystal polymer electrolytes [117]. Generally, it appears that insufficient oxidative stability of the electrolytes permitting a reversible cycling of metallic magnesium is the reason for their frequent incompatibility with the positive electrode [3].

Table 6
Transition metal borides used for chemical (c) and electrochemical (ec) insertion of magnesium ions[a]

Positive electrode material	Molecular weight	x_{max} in Mg_xMB_2 and experimental details			Ref.
		c[b]	ec	Electrolyte	
MoB_2	117.56	0.66	0.66	1 M $Mg(ClO_4)_2$/THF	[3]
TiB_2	69.52	0.42	0.42	1 M $Mg(ClO_4)_2$/THF	[3]
ZrB_2	112.84	0.66	0.66	1 M $Mg(ClO_4)_2$/THF	[3]

[a] c, chemical insertion; ec, electrochemical insertion; THF, tetrahydrofuran.
[b] Di-*n*-butylmagnesium as reagent.

5. Mechanistic aspects of Mg^{2+} insertion

Relative to Li^+ insertion into layered or channeled host materials, the insertion of Mg^{2+} ions needs a much higher activation energy for the heterogeneous insertion process at the surface of the host material and, normally, also for the diffusion process in the bulk of the host material. The doubly charged Mg^{2+} ion tends to coordinate both polar solvent molecules and anions present in the electrolyte solution to compensate its charge. Only highly polar solvents deliver enough solvation energy to overcome the dissociation energy necessary to form Mg^{2+} ions from salt molecules. In fact, in aqueous solutions Mg salts are dissociated and are very likely to form $[Mg(H_2O)_6]^{2+}$ when only the primary hydration shell is considered [118]. However, a value of 10–13 for the hydration number of Mg^{2+} ions was measured by the mobility method [119].

Generally, before Mg^{2+} ions can be inserted into a host lattice, at least part of their solvation sheath and coordinated anions have to be stripped off at the surface of the host material, which is reflected in a high activation energy for Mg^{2+} ion insertion into the lattice of the host material. Once the doubly charged ion is incorporated in the lattice it tends to stay at lattice places where the positive charges can be compensated best, thus, the Mg^{2+} ions remain close to two negative charges in the lattice. This implies that the doubly charged ion is retained much more strongly than a singly charged ion and, thus, a higher activation energy is needed for the hopping of the ions from one site to another.

This difficulty can be overcome if the doubly charged ion stays partly solvated when it is inserted or if it is intercalated into layered structures which contain solvating molecules (e.g., into V_2O_5 xerogels containing single and/or double layers of H_2O molecules in the interlayer spaces of the oxide [120–122]). Generally, the solvating molecule may be water or another polar molecule. If the space available for insertion was sufficient, it probably would also be possible to use some bidentate ligands like ethylene glycole or ethylene diamine to shield some of the positive charge. Another possibility is the insertion of singly charged Mg compounds, e.g., partly dissociated Mg salts or metal-organic compounds, e.g., MgF^+ or RMg^+ ions. In principle it would also be possible to insert Mg(I) ions, but normally such compounds are not stable enough. It may also be possible to chemically insert undissociated neutral Mg salts, but since there is no change in valence state of the elements in the host lattice upon insertion/de-insertion of such species, this is not of interest for charge storage devices. Most of the possibilities suggested above have not been tested experimentally as yet. Thus, a large domain remains to be searched in this field.

Probably the host most extensively investigated for Mg^{2+} insertion is V_2O_5. As an oversimplification, V_2O_5 can be regarded as a layered intercalation material (Fig. 2) similar to TiS_2 [65]. We therefore use the experimental results of Mg^{2+} intercalation into V_2O_5 to discuss some general aspects of the electrochemical Mg^{2+} intercalation into layered hosts. It has been found that traces of water play an important role in the intercalation process of Mg^{2+} into V_2O_5 [56]. Only very low specific charge could be achieved when V_2O_5 electrodes were cycled in fairly dry (< 1000 ppm H_2O) AN, PC, and tri-ethyleneglycole-dimethylether (triglyme) based electrolytes. Significantly higher specific charge was obtained when the water content in the solvent was increased [56] but it is not clear if water molecules were co-intercalated with magnesium ions or intercalated before the actual magnesium intercalation. In Fig. 9, the specific charge determined from the cathodic part (electrochemical insertion process) of the first voltammetric cycle of a V_2O_5 electrode is shown as a function of H_2O concentration in 1 M $Mg(ClO_4)_2 + x$ M H_2O/AN solutions. The specific charge increases with the water concentration in the electrolyte. The highest specific charge (more than 170 Ah/kg corresponding to 1.15 electrons per V_2O_5 unit for the best samples) was attained with ca 1 M H_2O in AN (Fig. 9). Note that this H_2O concentration is equal to the concentration of Mg^{2+} in the electrolyte. At higher H_2O levels, the specific charge of the V_2O_5 electrode decreases again. When lower Mg^{2+} concentrations were used the specific charge decreased, but

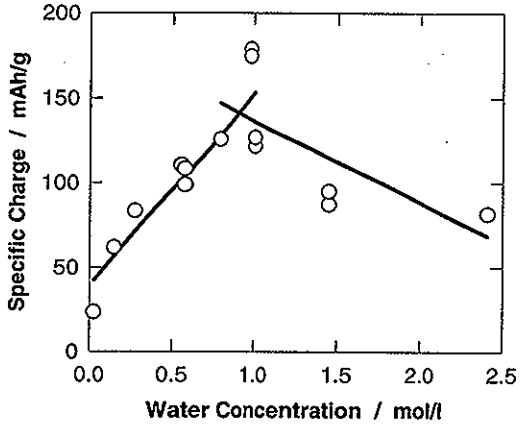

Fig. 9. The specific charge from the first voltammetric cycle for the electrochemical Mg^{2+} insertion into V_2O_5 as a function of H_2O concentration in the electrolyte 1 M $Mg(ClO_4)_2$ in acetonitrile [56].

again it had a maximum where the Mg^{2+}/H_2O molar ratio was about 1 [56]. An enhancement of the specific charge was observed also in propylene carbonate when H_2O was added to the dry electrolyte solution. In this case, however, a specific charge of only approximately 20 Ah/kg was reached in the wet electrolyte. Nearly the same behavior was observed also during experiments in triglyme-based electrolytes [56]. Thus, it can be concluded that the electrochemical magnesium insertion process obviously depends on the ratio between $c(H_2O)$ and $c(Mg^{2+})$ as well as on the absolute amount of H_2O in the solution.

Among the electrolytes tested hitherto the acetonitrile/H_2O mixture seems to be a good solvating agent which allows the Mg salt to dissociate with a flexible solvation shell which can be stripped off upon insertion. However, some water probably remains coordinated and, thus, is inserted together with the Mg^{2+} ion. This is supported by the observation that a V_2O_5-containing electrode which was reduced in 1 M $Mg(ClO_4)_2$ + 1 M H_2O/AN electrolyte and then transferred to a dry 1 M $Mg(ClO_4)_2$/AN solution gave the same anodic (Mg^{2+} de-insertion) charge as measured in the original wet electrolyte, whereas only poor electrochemical performance, typical for experiments in dry electrolytes, was observed during a subsequent reduction half-cycle. It is also known that polar molecules (e.g., H_2O) are taken up along with cations into the interlayer space in the case of layered sulfides [123]. On re-oxidation the exchangeable cations leave the interlayer space simultaneously with the water molecules [124]. The amount of H_2O taken into the interlayer space depends on the hydration energy and geometry of the cation [125].

Trace amounts of H_2O are expected to solvate small, highly-charged ions more effectively than organic solvents [126]. Indeed, low-temperature NMR experiments showed that preferential solvation of Mg^{2+} ions by H_2O molecules takes place in acetone solutions [127]. Hydration numbers of 6 for the Mg^{2+} ion were found irrespective of the solvent composition for $Mg(ClO_4)_2$ dissolved in acetone containing various amounts of H_2O molecules, and similarly in acetonitrile at temperatures between −90 and +60°C [127–130]. A preferential solvation of Mg^{2+} ions by H_2O molecules is thus expected as well in wet AN-based electrolytes.

When organic solvents are co-intercalated instead of H_2O into layered structures the products show interlayer spacings in most cases exceeding those found for hydrates [123]. Thus, taking into account that (i) less pronounced structural changes are occurring upon insertion of H_2O solvated cations and, (ii) the volume of the solvation shell is much smaller for cations solvated by H_2O than by organic solvents [131], one can conclude that water might facilitate cathodic insertion of ions into layered structures. This may explain the enhancement of the specific charge observed in H_2O-containing electrolytes.

At higher $Mg(ClO_4)_2$ concentrations ion pairs are formed. Just before the solubility limit is reached (ca 1.1 M $Mg(ClO_4)_2$ in the AN solvent) the number of ion pairs is expected to be considerable [126]. It has been shown by an analysis of infrared spectra that the $MgClO_4^+$ ion pair interacts strongly with only one acetonitrile molecule [129,130], while single Mg^{2+} ions are strongly solvated by six solvent molecules [127–130]. Since the solvated ion or ion pair is expected to shed at least part of its solvation shell before insertion into the oxide at the electrolyte/oxide interface, it is reasonable to assume that this process is simplified for the less solvated ion pairs. Therefore, one might assume that at high $Mg(ClO_4)_2$ concentrations $MgClO_4^+$ species could be inserted into V_2O_5 instead of, or together with Mg^{2+}. However, Novák and Desilvestro [56] found by atomic emission analysis that roughly two electrons were transferred per inserted magnesium. Thus, the insertion of ion pairs can probably be neglected.

It should be noted that the increase of specific charge with the H_2O content could also be explained by the incorporation of hydrogen atoms instead of Mg^{2+} ions into the V_2O_5 lattice, which in fact was proposed by Newby and Scott for aqueous acidic electrolytes [132]. However, the above atomic emission analysis [56] revealed that within experimental error, the magnesium content in the reduced oxide corresponds to the number of coulombs passed upon insertion. Thus, it can be concluded that the contribution of proton insertion to the overall electrochemical reaction is not significant.

Finally, it should be noted that an X-ray investigation [72] of electrochemical Mg^{2+} insertion into V_2O_5-based electrodes showed the insertion process to be complex and rather nonuniform. At least two new phases (possibly both of them $Mg_xV_2O_5$ phases) are formed in wet $Mg(ClO_4)_2$/AN electrolytes, however, the amount of one of them decreases during electrochemical cycling. Upon re-oxidation the original V_2O_5 structure is restored. Scanning electron microscopy of V_2O_5 single crystals after chemical (by interaction with a dibutylmagnesium solution) and electrochemical Mg^{2+} insertion [73] showed some morphology changes. Moreover, the individual crystals lost their single-crystal properties after electrochemical Mg^{2+} insertion. The structural data obtained from samples after chemical Mg^{2+} insertion suggest that only a small amount of Mg (about 1%) is located in the bulk V_2O_5 while the surface of the single crystal contains much more magnesium. It is therefore not clear whether Mg^{2+} insertion and the corresponding redox process only proceed at the surface or in the first few atomic layers of the single crystals, which would imply

a significant dependence of the measured specific charge of polycrystalline V_2O_5 particles on their grain size and porosity, as well as on their surface morphology. It is evident that much more experimental work is needed to fully understand the rather complicated Mg^{2+} insertion process into metal oxides.

6. Complete cells

In the preceding text we critically reviewed research results relevant to the development of an ambient-temperature rechargeable magnesium battery based on organic electrolytes. In the majority of the published work either the negative *or* positive electrode is treated; it appears that the integration of the cathode and anode chemistries is the foremost challenge for battery developers. According to our best knowledge only Gregory et al. [3] and Hoffmann et al. [33] at The Dow Chemical Company demonstrated a complete cell capable of ambient temperature operation. Their laboratory cell with a charge storage capacity of 6.7 mAh contained Mg sheet as the negative electrode, a composite positive electrode based on Co_3O_4 (with 15 wt% carbon black for electronic conductivity and 10 wt% polytetrafluoroethylene binder), and 0.25 M magnesium dibutyldiphenylborate in a THF/DME (vol. 7:3) mixture as the electrolyte. Four cycles with a coulombic efficiency of 99% and a cathode utilization of 86% were demonstrated. The cell voltage was slightly above 2 V during charging and approximately 0.6 V on discharge. The authors suggested that the high polarization could have been caused by low electrolyte concentration and/or poor ionization in the low-dielectric-constant solvent, and could probably be lessened by a different cell design and electrode structure, as well as by addition of supporting electrolytes. Furthermore, the authors observed that the electrolyte darkened during the test and probably underwent some decomposition. Hence, it is clear that all cell components and in particular the electrolyte require significant improvement. Nevertheless, the pioneering work of Gregory et al. [3] and Hoffmann et al. [33] demonstrated that a secondary battery of the type Mg/organic electrolyte/insertion cathode is technically feasible.

7. Conclusions

The reversible negative magnesium-metal electrode was scarcely investigated and is still poorly understood. For the positive electrode only a few oxidic insertion materials have been shown to reversibly accommodate Mg^{2+} ions. Starting with a specific charge of roughly 200 Ah/kg, after several tens of insertion/de-insertion cycles a specific charge of only ca 50 Ah/kg is realistic with the oxide V_2O_5, while ca 60–80 and 50 Ah/kg were demonstrated with hydrated vanadium bronzes and MoO_3, respectively. The mixed oxide $Mn_{2.15}Co_{0.37}O_4$ yields a specific charge of ca 30 Ah/kg. Water molecules present in the electrolyte facilitate the Mg^{2+} insertion into the oxides but, at the same time, do harm to the negative magnesium electrode. Thus, considerable improvement is needed before a competitive rechargeable magnesium-based battery will be realized.

Acknowledgements

Our work on magnesium insertion systems has been financed in part by the Swiss Federal Office of Energy, Bern.

References

[1] M.S. Vreeke, D.T. Mah, C.M. Doyle, J. Electrochem. Soc. 145 (1998) 3668.
[2] Chemical Market Reporter, Vol. 254, No. 2, p. 54, 1998.
[3] T.D. Gregory, R.J. Hoffman, R.C. Winterton, J. Electrochem. Soc. 137 (1990) 775.
[4] L.P. Lossius, F. Emmenegger, Electrochim. Acta 41 (1996) 445.
[5] K. Brandt, Solid State Ionics 69 (1994) 173.
[6] K. Brandt, J. Power Sources 54 (1995) 151.
[7] J.R. Dahn, A.K. Sleigh, H. Shi, B.M. Way, W.J. Weydanz, J.N. Reimers, Q. Zhong, U. von Sacken, in: G. Pistoia (Ed.), Lithium Batteries. New Materials, Developments and Perspectives, Elsevier, Amsterdam, 1994, p. 1.
[8] D. Aurbach, A. Schechter, M. Moshkovich, Z. Lu, Poster III Fri 81, in: Proceedings of Ninth International Meeting on Lithium Batteries, Edinburgh, UK, 12–17 July, 1998.
[9] V. Di Noto, M. Fauri, G. De Luca, M. Vidali, Poster III Fri 70, in: Proceedings of Ninth International Meeting on Lithium Batteries, Edinburgh, UK, 12–17 July, 1998.
[10] J.H. Connor, W.E. Reid Jr, G.B. Wood, J. Electrochem. Soc. 104 (1957) 38.
[11] S. Jayakrishnan, M. Pushpavanam, B.A. Shenoi, Surf. Technol. 13 (1981) 225.
[12] D.M. Overcash, F.C. Mathers, Trans. Electrochem. Soc. 64 (1933) 305.
[13] E. Findl, M.A. Ahmadi, K. Lul, US Patent No. 3 520 780, (1970).
[14] A. Brenner, J.L. Sligh, Trans. Institute of Met. Finish. 49 (1971) 71.
[15] J.D. Genders, D. Pletcher, J. Electroanal. Chem. 199 (1986) 93.
[16] A. Mayer, US Patent No. 4 778 575, (1988).
[17] C. Liebenow, J. Appl. Electrochem. 27 (1997) 221.

[18] A. Brenner, J. Electrochem. Soc. 118 (1971) 99.
[19] A. Brenner, Adv. Electrochem. Electrochem. Eng. 5 (1967) 205.
[20] A. Mayer, J. Electrochem. Soc. 137 (1990) 2806.
[21] J. Eckert, Dechema-Monographie 125 (1992) 425.
[22] J. Eckert, K. Gneupel, German (GDR) Patent No. DD 243 722 A1, (1987).
[23] W. Vonau, F. Berthold, J. Prakt. Chem. 336 (1994) 140.
[24] W.E. Elliott, J.R. Huff, R.W. Adler, W.L. Towle Proceedings of 20th Annual Power Sources Conference, 1966. p. 67.
[25] Y. Takada, Y. Miyake, Denki Kagaku 41 (1973) 62.
[26] V.Z. Leger, G.E. Blomgren, US Patent No. 4 142 028, (1979).
[27] S. Herrmann, M. Berthold, H. Kaden, Oberfläche-Surface 29 (1988) 15.
[28] T. Saito, H. Ikeda, Y. Matsuda, H. Tamura, J. Appl. Electrochem. 6 (1976) 85.
[29] M. Shibata, D. Omori, N. Furuya, Denki Kagaku 66 (1998) 411.
[30] G.G. Perrault, in: A.J. Bard (Ed.), Encyclopedia of Electrochemistry of the Elements. Marcel Dekker, New York, 1978. VIII. p. 263.
[31] A.N. Dey, J. Electrochem. Soc. 118 (1971) 1547.
[32] O.R. Brown, R. McIntyre, Electrochim. Acta 30 (1985) 627.
[33] R.J. Hoffmann, R.C. Winterton, T.D. Gregory, US Patent No. 4 894 302, (1990).
[34] L.P. Lossius, F.P. Emmenegger, Investigation of organic solvents for a magnesium based secondary battery, Internal report, Université de Fribourg, Switzerland, (1993).
[35] I.A. Kedrinsky, I.V. Murygin, V.E. Dmitrenko, O.E. Abolin, G.I. Sukhova, I.I. Grudyancev, J. Power Sources 22 (1988) 99.
[36] M.H. Miles, K.H. Park, D.E. Stilwell, J. Electrochem. Soc. 137 (1990) 3393.
[37] G.G. Kumar, N. Munichandraiah, Electrochim. Acta 44 (1999) 2663.
[38] M. Armand, D. Baril, Conference on 'Polymer Ionics', Gothenburg, Sweden, August 19–21, 1992. Oral presentation.
[39] Z. Ogumi, M. Inaba, Bull. Chem. Soc. Jpn 71 (1998) 521.
[40] M. Winter, J.O. Besenhard, M.E. Spahr, P. Novák, Adv. Mater. 10 (1998) 725.
[41] P. Novák, Annual project report for the Swiss Federal Office of Energy, Project No. EF-PROCC(91)018, Paul Scherrer Institute, Villigen, Switzerland, 1992.
[42] Y. Maeda, P. Touzain, L. Bonnetain, Synth. Met. 24 (1988) 267.
[43] Y. Maeda, P. Touzain, Electrochim. Acta 33 (1988) 1493.
[44] J.O. Besenhard, in: W. Müller-Warmuth, R. Schöllhorn (Eds.), Progress in Intercalation Research, Kluwer Academic Publishers, Dordrecht, 1994, p. 457.
[45] O. Yamamoto, Z. Ogumi, M. Morita, (Eds.), Proceedings of the Eighth International Meeting on Lithium Batteries, Nagoya, Japan, 16–21 June 1996. Elsevier, Amsterdam, 1997. Published as J. Power Sources, Vol. 68 (1997).
[46] Book of Abstracts, Proceedings of Ninth International Meeting on Lithium Batteries, Edinburgh, UK, 12–17 July, 1998.
[47] G. Pistoia (Ed.), Lithium Batteries. New Materials, Developments and Perspectives, Elsevier. Amsterdam, 1994.
[48] D.B. Le, S. Passerini, F. Coustier, J. Guo, T. Soderstrom, B.B. Owens, W.H. Smyrl, Chem. Mater. 10 (1998) 682.
[49] M.S. Whittingham, Prog. Solid State Chem. 12 (1978) 41.
[50] D.W. Murphy, J.N. Carides, F.J. Di Salvo, C. Cros, J.V. Waszczak, Mater. Res. Bull. 12 (1977) 825.
[51] A.J. Jacobson, R.R. Chilannelli, M.S. Whittingham, J. Electrochem. Soc. 12 (1979) 2277.
[52] M.B. Dines, Mater. Res. Bull. 10 (1975) 287.
[53] P.G. Bruce, F. Krok, J. Nowinski, V.C. Gibson, K. Tavakkoli, J. Mater. Chem. 1 (1991) 705.
[54] P.G. Bruce, F. Krok, P. Lightfoot, J.L. Nowinski, V.C. Gibson, Solid State Ionics 53 (1992) 351.
[55] P. Lightfoot, F. Krok, J.L. Nowinski, P.G. Bruce, J. Mater. Chem. 2 (1992) 139.
[56] P. Novák, J. Desilvestro, J. Electrochem. Soc. 140 (1993) 140.
[57] P. Novák, Final project report for the Swiss Federal Office of Energy, Project No. EF-PROCC(91)018, Paul Scherrer Institute, Villigen, Switzerland, 1994.
[58] R.R. Chianelli, M.B. Dines, Inorg. Chem. 14 (1975) 2417.
[59] D.W. Murphy, F.A. Trumbore, J. Cryst. Growth 39 (1977) 185.
[60] J. Rijnsdorp, F. Jellinek, J. Solid State Chem. 25 (1978) 325.
[61] S. Kikkawa, N. Ogawa, M. Koizumi, J. Solid State Chem. 41 (1982) 315.
[62] T. Yamamoto, S. Kikkawa, M. Koizumi, J. Electrochem. Soc. 133 (1986) 1558.
[63] W. Yuan, J.R. Günter, Solid State Ionics 76 (1995) 253.
[64] C. Delmas, in: G. Pistoia (Ed.), Lithium Batteries. New Materials, Developments and Perspectives, Elsevier, Amsterdam, 1994, p. 457.
[65] P.G. Dickens, M.F. Pye, in: M.S. Whittingham, A.J. Jacobson (Eds.), Intercalation Chemistry, Academic Press, Inc, NY, USA, 1982, p. 547.
[66] D.W. Murphy, P.A. Christian, F.J. Di Salvo, J.V. Waszczak, Inorg. Chem. 18 (1979) 2800.
[67] M.S. Whittingham, J. Electrochem. Soc. 123 (1975) 315.
[68] J.M. Cocciantelli, J.P. Doumerc, M. Pouchard, M. Broussely, J. Labat, J. Power Sources 34 (1991) 103.
[69] J. Labat, J.M. Cocciantelli, French Patent No. 8 916 337, (1989).
[70] C. Delmas, H. Cognac-Auradou, J.M. Cocciantelli, M. Ménétrier, J.P. Doumerc, Solid State Ionics 69 (1994) 257.
[71] J.P. Pereira-Ramos, R. Messina, J. Perichon, J. Electroanal. Chem. 218 (1987) 241.

[72] P. Novák, V. Shklover, R. Nesper, Z. Phys. Chem. 185 (1994) 51.
[73] V. Shklover, T. Haibach, F. Ried, R. Nesper, P. Novák, J. Solid State Chem. 123 (1996) 317.
[74] J. Galy, M. Pouchard, Bull. Soc. Chi. Fr., (1967) 261.
[75] J. Galy, M. Pouchard, A. Casalot, P. Hagenmuller, Bull. Soc. Fr. Mineralogr. Cristallogr., (1967) 544.
[76] K. West, B. Zachau-Christiansen, M.J.L. Ostergard, T. Jacobsen, J. Power Sources 20 (1987) 165.
[77] K. Salloux, F. Chaput, H.P. Wong, B. Dunn, M.W. Breiter, J. Electrochem. Soc. 142 (1995) L191.
[78] D.B. Le, S. Passerini, A.L. Tipton, B.B. Owens, W.H. Smyrl, J. Electrochem. Soc. 142 (1995) L102.
[79] D.B. Le, S. Passerini, J. Guo, J. Ressler, B.B. Owens, W.H. Smyrl, J. Electrochem. Soc. 143 (1996) 2099.
[80] K. West, B. Zachau-Christiansen, T. Jacobsen, S. Skaarup, Electrochim. Acta 38 (1993) 1215.
[81] L. Abello, C. Pommier, J. Chimie Physique 80 (1983) 373.
[82] A. Bouhaouss, P. Aldebert, N. Baffier, J. Livage, Rev. Chim. Minerale 22 (1985) 417.
[83] D.W. Murphy, P.A. Christian, F.J. DiSalvo, J.N. Carides, J. Electrochem. Soc. 126 (1979) 497.
[84] D.W. Murphy, P.A. Christian, F.J. DiSalvo, J.N. Carides, J.V. Waszcsak, J. Electrochem. Soc. 128 (1981) 2053.
[85] K. West, B. Zachau-Christiansen, T. Jacobsen, Electrochim. Acta 28 (1983) 1829.
[86] K.M. Abraham, J.L. Goldmann, M.D. Dempsey, J. Electrochem. Soc. 128 (1981) 2493.
[87] F.B. Joho, PhD thesis No. 11745, ETH Zurich, Switzerland, (1996).
[88] F. Joho, P. Novák, O. Haas, R. Nesper, Chimia 47 (1993) 288.
[89] K. Nassau, D.W. Murphy, J. Non-Cryst. Solids 44 (1981) 297.
[90] M. Pasquali, G. Pistoia, V. Manev, R.V. Moshtev, J. Electrochem. Soc. 133 (1986) 2454.
[91] A. Momchilov, V. Manev, A. Nassalevska, M. Pasquali, G. Pistoia, J. Appl. Electrochem. 20 (1990) 763.
[92] G. Pistoia, L. Li, G. Wang, Electrochim. Acta 37 (1992) 63.
[93] V. Manev, A. Momchilov, A. Nassalevska, G. Pistoia, M. Pasquali, J. Power Sources 54 (1995) 501.
[94] P. Novák, W. Scheifele, O. Haas, Molten Salt Forum 1–2 (1993/94) 389.
[95] P. Novák, W. Scheifele, F. Joho, O. Haas, J. Electrochem. Soc. 142 (1995) 2544.
[96] P. Novák, W. Scheifele, O. Haas, J. Power Sources 54 (1995) 479.
[97] G. Pistoia, S. Panero, M. Tocci, R.V. Moshtev, V. Manev, Solid State Ionics 13 (1984) 311.
[98] M.E. Spahr, P. Novák, W. Scheifele, O. Haas, R. Nesper, J. Electrochem. Soc. 145 (1998) 421.
[99] G. Pistoia, M. Pasquali, M. Tocci, V. Manev, R.V. Moshtev, J. Power Sources 15 (1985) 13.
[100] L. Kihlborg, Ark. Kemi 21 (1963) 357.
[101] M.S. Whittingham, M.B. Dines, J. Electrochem. Soc. 124 (1977) 1387.
[102] T. Ohzuku, in: G. Pistoia (Ed.), Lithium Batteries. New Materials, Developments and Perspectives, Elsevier, Amsterdam, 1994, p. 256.
[103] L. Campanella, G. Pistoia, J. Electrochem. Soc. 118 (1971) 1905.
[104] P.G. Dickens, G.J. Reynolds, in: C.H.F. Barry, P.C.H. Mitchell (Eds.), Proceedings of Climax Molybdenum, Fourth International Conference on Chemistry and Uses of Molybdenum, Climax Molybdenum Co., Ann Arbor, MI, USA, 1982. p. 32.
[105] C.-G. Granqvist, Appl. Phys. A 57 (1993) 3.
[106] J.O. Besenhard, J. Heydecke, H.P. Fritz, Solid State Ionics 6 (1982) 215.
[107] J.O. Besenhard, J. Heydecke, E. Wudy, H.P. Fritz, W. Foag, Solid State Ionics 8 (1983) 61.
[108] J.O. Besenhard, R. Schöllhorn, J. Power Sources 1 (1976/77) 267.
[109] M.E. Spahr, P. Novák, O. Haas, R. Nesper, J. Power Sources 54 (1995) 346.
[110] M.E. Spahr, PhD thesis No. 12281, ETH Zurich, Switzerland, (1997).
[111] L. Sánchez, J.-P. Pereira-Ramos, J. Mater. Chem. 7 (1997) 471.
[112] J. Farcy, J.-P. Pereira-Ramos, L. Hernán, J. Morales, J.L. Tirado, Electrochim. Acta 39 (1994) 339.
[113] L. Sánchez, J. Farcy, J.-P. Pereira-Ramos, L. Hernán, J. Morales, J.L. Tirado, J. Mater. Chem. 6 (1996) 37.
[114] B.O. Loopstra, Acta Cryst. 17 (1964) 651.
[115] R.E. Dueber, J.M. Fleetwood, P.G. Dickens, Solid State Ionics 50 (1992) 329.
[116] C. Liebenow, Electrochim. Acta 43 (1998) 1253.
[117] F.B. Dias, S.V. Batty, A. Gupta, G. Ungar, J.P. Voss, P.V. Wright, Electrochim. Acta 43 (1998) 1217.
[118] F.A. Cotton, G. Wilkinson, in: Advanced Inorganic Chemistry, Verlag Chemie, Weinheim/Bergstrasse, 1970 p. 402. Second edition, in German.
[119] J. Koryta, J. Dvořák, in: Principles of Electrochemistry, John Wiley and Sons, Chichester, 1987, p. 24.
[120] S. Kittaka, N. Uchida, T. Kihara, T. Suetsugi, T. Sasaki, Langmuir 8 (1992) 245.
[121] S. Kittaka, T. Suetsugi, S. Morikawa, N. Uchida, Langmuir 9 (1993) 1104.
[122] N. Baffier, L. Znaidi, J.C. Badot, J. Chem. Soc., Faraday Trans. 86 (1990) 2623.
[123] A. Lerf, R. Schöllhorn, Inorg. Chem. 16 (1977) 2950.
[124] R. Schöllhorn, W. Schmucker, Z. Naturforsch. 30b (1975) 975.
[125] R. Schöllhorn, E. Sick, A. Lerf, Mater. Res. Bull. 10 (1975) 1005.
[126] O.R. Brown, R. McIntyre, Electrochim. Acta 29 (1984) 995.
[127] A.D. Covington, A.K. Covington, J. Chem. Soc., Faraday Trans. 1 71 (1975) 831.
[128] I.S. Perelygin, M.A. Klimchuk, Russian J. Phys. Chem. 48 (1974) 1466.
[129] I.S. Perelygin, M.A. Klimchuk, Russian J. Phys. Chem. 47 (1973) 1138.
[130] I.S. Perelygin, M.A. Klimchuk, Russian J. Phys. Chem. 47 (1973) 1402.

[131] B.E. Conway, J.O'M. Bockris, in: J.O'M. Bockris, B.E. Conway, editors. Modern Aspects of Electrochemistry. Butterworths, London, 1954. 1. p. 63.
[132] K.R. Newby, A.B. Scott, J. Eletrochem. Scc. 117 (1970) 152.
[133] M.M. Thackeray, L.A. De Picciotto, A. de Kock, P.J. Johnson, V.A. Nicholas, K.T. Adendorff, J. Power Sources 21 (1987) 1.
[134] A. Yu, N. Kumagai, Z. Liu, J.Y. Lee, J. Solid State Electrochem. 2 (1998) 394.
[135] P.G. Dickens, D.J. Penny, M.T. Weller, Solid State Ionics 18–19 (1986) 778.